H/D fragment ratio in Lyman-α photolysis of CH_2D_2

Albert J. R. Heck
Combustion Research Facility, Sandia National Laboratories, Livermore, California 94551 and Department of Chemistry, Stanford University, Stanford, California 94305

Richard N. Zare
Department of Chemistry, Stanford University, Stanford, California 94305

David W. Chandler
Combustion Research Facility, Sandia National Laboratories, Livermore, California 94551

(Received 17 November 1995; accepted 25 December 1995)

The photofragment imaging technique is used to study the formation of H and D in the photolysis of CH_2D_2. From the images different reaction channels are distinguished that lead to hydrogen fragments. For the channel that leads to hydrogen atoms concomitant with methyl fragments a H/D ratio of 3.5 ± 0.6 is found. © *1996 American Institute of Physics.* [S0021-9606(96)03709-0]

INTRODUCTION

Methane photolysis is of interest in the atmospheres of the earth and other planets.[1,2] The first excited electronic state of methane is located approximately 8.7 eV above the ground state.[3,4] Therefore, the photochemistry of methane in the atmosphere is mostly driven by intense solar atomic emission lines, such as Lyman-α radiation. At photon energies corresponding to Lyman α only the lowest singlet, $^1T_2$, electronic state can be accessed. The $^1T_2$ electronic state is believed to have a short lifetime with respect to dissociation, which partly explains the observed broad and diffuse absorption band.[3,4] The $^1T_2$ state correlates adiabatically with the $^1CH_2$ $(^1B_1)$ + H_2 products.[5,6] A study by Mordaunt *et al.*[7] and our study on methane[8] revealed that the formation of methyl fragments concomitant with hydrogen atoms is the dominant channel in the Lyman-α photolysis of methane. Additionally, these studies indicated that at least one alternative channel produces hydrogen atoms in the VUV photolysis of methane.

In this paper we present results on the formation of H and D from the Lyman-α photolysis of CH_2D_2. The photofragment imaging technique[9,10] enables us to derive the relative contributions from the channels that lead to formation of H and/or D fragments from the photolysis of CH_2D_2. We find that the dominant channel (>80%) leads to hydrogen fragments concomitant with methyl fragments; an alternative channel proceeds via three-body dissociations, which lead to $CH+H+H_2$ fragments and/or CH_2+H+H fragments. We observe a significant preference for formation of H over D photofragments from the photolysis of CH_2D_2. The isotope effects are very different for the channels that lead to (a) H atoms concomitant with CH_3 fragments, and (b) H atoms concomitant with $CH+H_2$ and/or CH_2+H fragments. We compare this H/D isotope effect with the results from studies on other small polyatomics, such as water and triplet methylene, and note interesting similarities.

EXPERIMENT

The photofragment imaging apparatus has been described previously.[8,10] The experimental procedures used in this study and our previous study on the formation of H fragments from the photolysis of CH_4 (Ref. 8) are similar. Research grade CH_2D_2 (D_2 98%, Cambridge Isotope Laboratories, Andover, MA) was used without further purification.

H and D photofragments are observed when the combined VUV ($\lambda=121.6$ nm) and UV ($\lambda=365$ nm) laser beams intersect with the neat CH_2D_2 molecular beam. The $(1+1')$ resonance-enhanced multiphoton ionization (REMPI) transition frequencies for H and D atoms are slightly different. Therefore, the H or D photofragments can be mass-selectively ionized. The recorded H or D photofragment images are two-dimensional projections of the three-dimensional recoil of the ionized photofragments. The experimental configuration used dictates that the initial three-dimensional distribution has cylindrical symmetry and therefore the inverse Abel transform can be used to reconstruct the three-dimensional recoil of the photofragments.[10] Velocity distributions (speed and angle) are obtained from the inverse Abel transformed image.[10]

RESULTS

In Fig. 1 a REMPI spectrum of the atomic photofragments from CH_2D_2 is shown, for which the laser is scanned over a wavelength range that includes the H and D transitions, while collecting all ions with masses between 0.1 and 5. The signals are centered around 121.53 nm and 121.57 nm correspond with $m/z=2$ signal (D atoms) and $m/z=1$ (H atoms), respectively. By integrating these ion signals separately we find that the σ_H/σ_D branching ratio is 3.0 for this particular scan. From a series of 8 repeated scans an averaged σ_H/σ_D value of 3.1 ± 0.5 is found. When the molecular beam is not fired, a small (less than 2%) H-atom background signal is observed (no significant D-atom background signal), which is neglected. To extract quantitative data from these ion spectra care is taken that the UV laser power is constant over the wavelength range scanned. Although frequency tripling in a phase-matched Kr/Ar mixture is bandwidth limited, our experimental arrangement (the length of the tripling cell and focal length of the used lens being im-

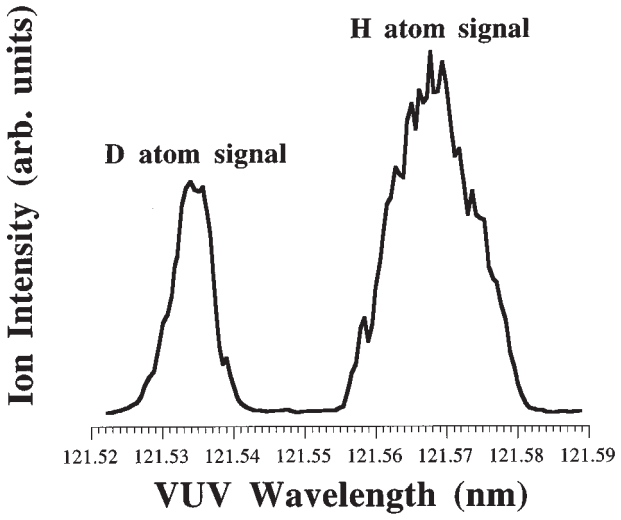

FIG. 1. REMPI spectrum of the atomic photofragments from the Lyman-α photolysis of CH_2D_2. The laser is scanned over the 121.52 to 121.59 nm wavelength range, which includes H and D transitions. The signal centered around 121.53 nm corresponds to $m/z=2$ signal (D atoms), the signal centered near 121.57 nm corresponds to $m/z=1$ (H atoms). By integrating these ion signals a σ_H/σ_D branching ratio of 3.0 is found for this particular scan.

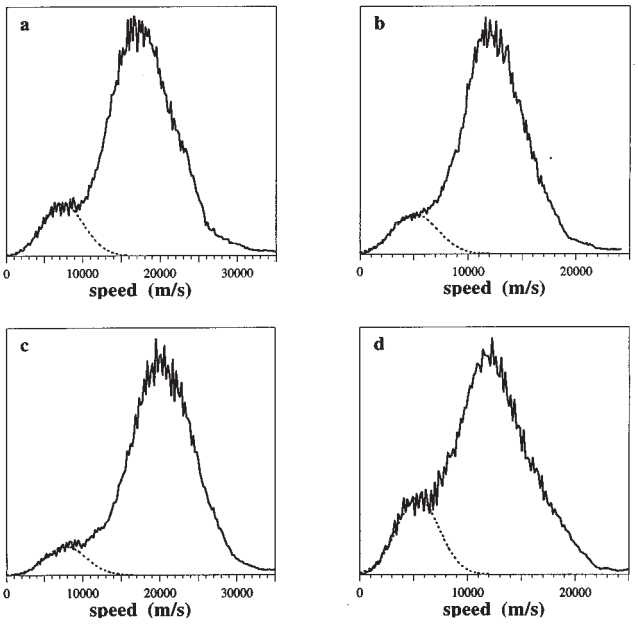

FIG. 2. Speed distributions of atomic hydrogen photofragments following absorption of a Lyman-α photon in methane. (a) H-photofragments of CH_4. (b) D-photofragments of CD_4. (c) H-photofragments of CH_2D_2. (d) D-photofragments of CH_2D_2.

portant parameters) ensures that the generated VUV power is constant over the 0.07 nm VUV wavelength range scanned.[11] Nonetheless, scans were taken with the Ar/Kr mixture optimized on the H, and alternatively the D ion signals. This procedure leads to similar σ_H/σ_D branching ratios.

Additionally, we measured images of H and D photofragments from the photolysis of CH_2D_2. These photofragment images are recorded while the laser is scanned over the entire H or D atom Doppler profiles. An H-atom photofragment image of the Lyman-α photolysis of CH_4 has been presented previously.[8] Qualitatively, the recorded H and D photofragment images of the photolysis of CH_2D_2 are similar to the photofragment image of the H-atom photofragments from the Lyman-α photolysis of CH_4. Two distinct rings are observed in all images—the inner one is isotropic and the outer one anisotropic. Figures 2(a)–(d) show the speed distributions of the hydrogen-atom photofragments following the photolysis of CH_2D_2 [Figs. 2(c) and 2(d)], and, for comparison, CH_4 [Fig. 2(a)] and CD_4 [Fig. 2(b)]. These speed distributions show the two distinct channels that lead to hydrogen atoms in the photolysis of methane.

DISCUSSION

Ion images

The fast channel observed in the photofragment images can only be attributed[8] to hydrogen atoms formed concomitant with methyl fragments,

$$\text{(I)}\quad CH_4(^1A_1)\rightarrow CH_3(^2A_{2''})+H,\quad \Delta E=4.48\ \text{eV}.$$

Absorption of a Lyman-α photon deposits approximately 10.2 eV in the methane molecules, which leaves 5.7 eV available for translational excitation of the H and CH_3 photofragments, and/or internal excitation of the CH_3 fragment. This excess energy corresponds to a maximum speed of the H photofragments of approximately 32 km/s. This speed is indeed the maximum observed [see Figs. 2(a) and 2(c)]. Similarly, the maximum expected, and observed, speeds of the D photofragments are approximately 22 km/s [see Figs. 2(b) and 2(d)].

The angular distributions of the H and D atomic photofragments in the outer ring of the images of CH_2D_2 were fit to

$$I(\theta)\approx 1+\beta_2 P_2(\cos\theta),$$

where $P_2(\cos\theta)$ is the second-order Legendre polynomial and β_2 is the anisotropy parameter.[12] The resulting anisotropy parameters are compared to those for CH_4 and CD_4 in Table I. The anisotropy parameters range between 0.20 and 0.28, which indicates that the excited methane molecules have a relatively short lifetime prior to dissociation via this channel and that the transition has predominately parallel character.

The mechanism that leads to the slower hydrogen atoms cannot be assigned unambiguously. Contributions from the following channels are possible:

TABLE I. Branching ratios of the slow and fast channel, and anisotropy parameter for the fast channel in the H/D photofragment images.

Parent	Fragment	% Slow channel	% Fast channel	β Fast channel
CH_4	H	13	87	0.28
CH_2D_2	H	8	92	0.25
CH_2D_2	D	19	81	0.25
CD_4	D	12	88	0.20

TABLE II. Branching ratios (σ_H/σ_D) in the photolysis of CH_2D_2.

	σ_H/σ_D	Assignment
Integrated	3.1±0.5	total yield of H/D atoms
Slow channel	1.3±0.4	$CH_4 \rightarrow CH_2+H+H$ and/or $CH_4 \rightarrow CH+H_2+H$
Fast channel	3.5±0.6	$CH_4 \rightarrow CH_3+H$

(II) $CH_4(^1A_1) \rightarrow CH_2(^3B_1)+H+H, \quad \Delta E = 9.21$ eV

(III) $CH_4(^1A_1) \rightarrow CH_2(a\ ^1A_1)+H+H, \quad \Delta E = 9.48$ eV

(IV) $CH_4(^1A_1) \rightarrow CH(^2\Pi)+H_2+H, \quad \Delta E = 9.07$ eV.

Here ΔE is the energy required for each particular channel.[13] Although we cannot assign the mechanism(s) that leads to the slower H atoms unambiguously, our previous study on the photolysis of methane[8] revealed that channel IV contributes significantly to the formation of H_2 photofragments from the photolysis of methane. That observation implies that this channel is responsible for at least part of the slow hydrogen photofragments observed in the images.

The contributions from the fast channel (CH_3+H) and slow channel (CH_2+H+H, and/or $CH+H_2+H$) to the images is obtained by fitting the slow channel in the speed distributions to a Gaussian function. This seems to be a reasonable fit function as it describes the slower, leading edge of the speed distributions well [see Figs. 2(a)–2(d)]. The relative contributions of the slow and fast channels to the H and D photofragments images are given in Table I. Figure 2 and Table I show that the relative contribution of the slow and fast channels are quantitatively similar for the H photofragments from CH_4 and the D photofragments from CD_4, i.e., approximately 87% of the hydrogen photofragments in the images are formed via channel I. For CH_2D_2, however, the relative contributions to the H and D images from channel I are quite different, i.e., 92% for the H image, and 81% for the D image.

Isotope effect in the photolysis of CH_2D_2

The integrated, relative yield of H and D photofragments from the photolysis of CH_2D_2 is obtained from the REMPI scans (Fig. 1), and is 3.1±0.5. Our H and D photofragment images reveal, however, that different channels contribute to the formation of hydrogen atoms from the photolysis of methane. Using the photofragment imaging technique we can distinguish these channels, and derive their relative importance (see Table I), and obtain the σ_H/σ_D branching ratios for the different channels (see Table II). We find that the $CH_2D_2 \rightarrow CHD_2+H$ channel is favored over the $CH_2D_2 \rightarrow CH_2D+D$ by a factor 3.5±0.6. In the formation of hydrogen atoms via the combined channels II, III, and IV, the H over D ratio is much smaller, i.e., 1.3±0.4. Owing to the difficulty in assigning this channel we will not discuss it further here.

We consider the isotope effect observed in channel I as this channel is unambiguously assigned. The minimum energy path for breaking the CH_3–H bond in methane has been calculated and exhibits no activation barrier.[14,15] The energetic threshold for this channel is only 4.48 eV. Therefore, excitation of methane at Lyman α brings the molecule high above the energetic threshold for formation of atomic hydrogen photofragments. Additionally, excitation at Lyman α is approximately 1.5 eV higher in energy than the bandhead of the first absorption band of methane.[4] The large isotope effect may seem at first to be somewhat surprising, but it is not unprecedented. Studies on other small polyatomics have revealed large H/D isotope effects.[16]

Selective photolytic X–H/X–D bond breaking has been demonstrated experimentally and predicted theoretically for small molecules such as water,[17–22] triplet methylene,[23] acetylene,[24] and ethylene.[25] These studies reveal that, in general, the σ_H/σ_D branching ratios depend on the excitation energy, and the initial state of the molecules. Although the largest isotope effects are predicted to occur when the excitation is at the leading, low-energy part of the absorption band, recent theoretical calculations also predict large isotope effects when the excitation is significantly shifted to higher energies.[17–20,23] A similar feature was found in the correlation between σ_H/σ_D branching ratio and the excitation energy in theoretical studies on both HOD (Refs. 17–20) and triplet CHD (Ref. 23). The σ_H/σ_D branching ratio is calculated to be very high (>10) for excitation energies corresponding to the low energy side of the absorption spectrum. The σ_H/σ_D branching ratio drops to approximately 2 at ''intermediate'' excitation energies, but increases again at even higher excitation energies. The HOD dissociation has been studied experimentally[21] and modeled theoretically following absorption of a 157 nm photon.[18–20] This radiation excites the HOD molecule approximately 1.1 eV above the bandhead of the absorption band and 2.8 eV above the energetic threshold for dissociation. A σ_H/σ_D branching ratio of 4 is observed[21] and theoretically predicted.[18,20] Similarly, calculations predict a σ_H/σ_D branching ratio of 12 when triplet CHD is excited 1.5 eV above the bandhead of the absorption band, i.e., 2.6 eV above the dissociation threshold.[23] In our experiments methane is excited 1.5 eV above the leading edge of the absorption spectrum and 5.7 eV above the threshold for dissociation. We observe a σ_H/σ_D branching ratio of 3.5±0.6 for the channel that produces hydrogen atoms concomitant with methyl fragments. The similarities observed in these different systems are quite remarkable.

The observed σ_H/σ_D branching ratio isotope effect of 3.5±0.6 following absorption at Lyman α is certainly consistent with earlier studies. A more detailed interpretation of these isotope effects in the σ_H/σ_D branching ratio must

await a theoretical calculation of the methane (and CH_2D_2) dissociation dynamics on a reliable potential energy surface.

ACKNOWLEDGMENTS

This work was supported by the U.S. Department of Energy, Office of Basic Energy Sciences, Division of Chemical Sciences, and by the U.S. National Science Foundation under NSF.

[1] J. S. Levine, *The Photochemistry of Atmospheres* (Academic, New York, 1985).
[2] A. Sternberg and A. Dalgarno, Astrophys. J. **99**, 565 (1995).
[3] M. B. Robin, *Higher Excited States of Polyatomic Molecules* (Academic, New York, 1974).
[4] L. C. Lee and C. C. Chiang, J. Chem. Phys. **78**, 688 (1983).
[5] S. Karplus and R. Bersohn, J. Chem. Phys. **51**, 2040 (1969).
[6] M. S. Gordon and J. W. Caldwell, J. Chem. Phys. **70**, 5503 (1979).
[7] D. H. Mordaunt, I. R. Lambert, G. P. Morley, M. N. R. Ashfold, R. N. Dixon, L. Schnieder, and K. H. Welge, J. Chem. Phys. **98**, 2054 (1993).
[8] A. J. R. Heck, R. N. Zare, and D. W. Chandler, J. Chem. Phys. (in press).
[9] D. W. Chandler and P. L. Houston, J. Chem. Phys. **87**, 1445 (1987).
[10] A. J. R. Heck and D. W. Chandler, Annu. Rev. Phys. Chem. **46**, 355 (1995).
[11] R. Mahon, T. J. McIlrath, V. P. Myerscough, and D. W. Koopman, IEEE J. Quant. Electron. **QE-15**, 444 (1979).
[12] R. N. Zare, Mol. Photochem. **4**, 1 (1972).
[13] S. G. Lias, J. E. Bartmess, J. F. Liebman, J. L. Holmes, R. D. Levin, and W. G. Mallard, J. Phys. Chem. Ref. Data. **17**, (1988).
[14] D. M. Hirst, Chem. Phys. Lett. **122**, 225 (1985).
[15] M. Sironi, D. L. Cooper, J. Gerratt, and M. Raimondi, J. Am. Chem. Soc. **112**, 5054 (1990).
[16] B. Katz and R. Bersohn, in *Isotope Effects in Gas Phase Chemistry*, edited by J. Kaye, ACS Series, 1992, Vol. 502, p. 66.
[17] O. Atabek, M. T. Bourgeois, and M. Jacon, J. Chem. Phys. **87**, 5870 (1987).
[18] V. Engel and R. Schinke, J. Chem. Phys. **88**, 6831 (1988).
[19] D. G. Imre and J. Zhang, Chem. Phys. **139**, 89 (1989).
[20] J. Zhang, D. G. Imre, and J. H. Frederick, J. Phys. Chem. **93**, 1840 (1989).
[21] N. Shafer, S. Satyapal, and R. Bersohn, J. Chem. Phys. **90**, 6807 (1989).
[22] R. L. Vander Wal, J. L. Scott, and F. F. Crim, J. Chem. Phys. **92**, 803 (1990).
[23] R. A. Beärda, G.-J. Kroes, M. C. van Hemert, B. Heumann, R. Schinke, and E. F. van Dishoeck, J. Chem. Phys. **100**, 11 113 (1994).
[24] T. A. Cool, P. M. Goodwin, and C. E. Otis, J. Chem. Phys. **93**, 3714 (1990).
[25] S. Satyapal, G. W. Johnston, and R. Bersohn, J. Chem. Phys. **93**, 6398 (1990).